

# Magnetometry with Mesospheric Sodium

J. M. Higbie,<sup>1,\*</sup> S. M. Rochester,<sup>2</sup> B. Patton,<sup>2</sup> R. Holzlohner,<sup>3</sup> D. Bonaccini Calia,<sup>3</sup> and D. Budker<sup>2,4,†</sup>

<sup>1</sup>*Department of Physics and Astronomy, Bucknell University, Lewisburg, PA 17837*

<sup>2</sup>*Department of Physics, University of California, Berkeley, CA 94720-7300*

<sup>3</sup>*European Southern Observatory (ESO), Garching bei München, D-85748, Germany*

<sup>4</sup>*Nuclear Science Division, Lawrence Berkeley National Laboratory, Berkeley CA 94720*

(Dated: Dec. 18, 2009)

Measurement of magnetic fields on the few-hundred-kilometer length scale is significant for a variety of geophysical applications including mapping of crustal magnetism and ocean-circulation measurements, yet available techniques for such measurements are very expensive or of limited accuracy. We propose a scheme for remote detection of magnetic fields using the naturally occurring atomic-sodium-rich layer in the mesosphere and existing high-power lasers developed for laser guide-star applications. The proposed scheme offers dramatic reduction in cost, opening the way to large-scale magnetic mapping missions.

## I. INTRODUCTION

Measurements of geomagnetic fields are an important tool for peering into the earth's interior, with measurements at differing spatial scales giving information about sources at corresponding depths. Measurements of fields on the few-meter scale can locate buried ferromagnetic objects (e.g. unexploded ordnance or abandoned vessels containing toxic waste), while maps of magnetic fields on the kilometer scale are used to locate geological formations promising for mineral or oil extraction. On the largest scale, the earth's dipole field gives information about the geodynamo at depths of several thousand kilometers. Magnetic measurements at intermediate length scales, in the range of several tens to several hundreds of kilometers likewise offer a window into important scientific phenomena, including the behavior of the outer mantle, the solar-quiet dynamo in the ionosphere [1], and ionic currents as probes of ocean circulation[2], a major actor in models of climate change.

To avoid contamination from local perturbations, magnetic-field measurements on this length scale must typically be made at a significant height above the earth's surface. Though magnetic mapping at high altitude has been realized with satellite-borne magnetic sensors [3, 4, 5], the great expense of multi-satellite missions places significant limitations on their deployment and use. Here we introduce a high-sensitivity method of measuring magnetic fields with 100-km spatial resolution without the cost of spaceborne apparatus, by exploiting the naturally occurring atomic sodium layer in the mesosphere and the significant technological infrastructure developed for astronomical laser guide stars (LGS). This method promises to enable creation of global sensor arrays for continuous mapping and monitoring of geomagnetic fields without interference from ground-based sources.

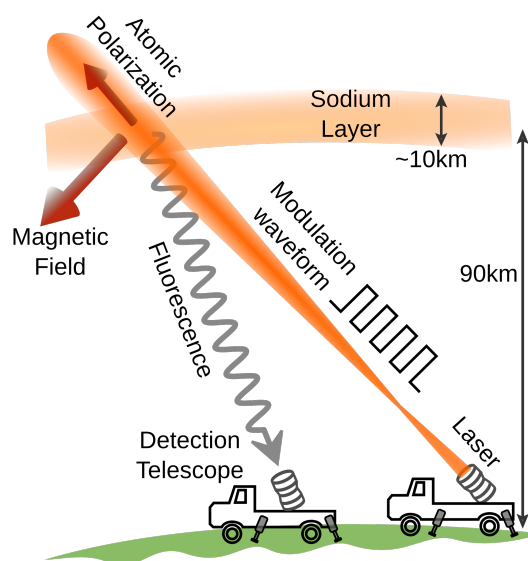


FIG. 1: Fluorescent detection of magneto-optical resonance of mesospheric sodium. (Diagram not to scale). Circularly polarized laser light at 589 nm, modulated near the Larmor frequency, pumps atoms in the mesosphere. The resulting spin polarization (pictured as instantaneously oriented along the laser beam propagation direction) precesses around the local magnetic field. Fluorescence collected by a detection telescope exhibits a resonant dependence on the modulation frequency.

## II. PRINCIPLE OF THE METHOD

The measurement we envisage is closely related to the techniques of atomic magnetometry, appropriately adapted to the conditions of the mesosphere. The principle of the method is to measure the magnetic field using spin precession of sodium atoms by creating atomic spin polarization, allowing it to evolve coherently in the magnetic field, and determining the post-evolution spin state. Conceptually, these processes are distinct and sequential, although in practice they may occur simultaneously and at different times for different atoms. Preparation of spin-polarized mesospheric sodium

\*Electronic address: james.higbie@bucknell.edu

†Electronic address: budker@berkeley.edu

atoms is achieved by optical pumping, as was proposed for mesospheric sodium in the seminal paper on sodium LGS by Happer et al. [6]. In the simplest realization, the pumping laser beam is circularly polarized and is launched from a telescope at an angle approximately perpendicular to the local magnetic field, as shown in Fig. 1. In the presence of the magnetic field, the transverse polarization generated by optical pumping precesses around the magnetic-field direction at the Larmor frequency. In order to avoid “smearing” of the atomic polarization due to this precession, the optical-pumping rate is modulated near the Larmor frequency, as first demonstrated by Bell and Bloom [7]. When the modulation frequency and the Larmor frequency coincide, a resonance results, and a substantial degree of atomic polarization is obtained. The atomic polarization in turn modifies the fluorescence from the sodium atoms, which can be detected by a ground-based telescope. This allows the sodium atoms to serve as a remote sensor of the magnitude of the magnetic field in the mesosphere, i.e. as a scalar magnetometer. By stationing lasers and detectors on a few-hundred-kilometer grid, a simultaneous map of magnetic fields may be obtained; alternatively, the laser and detector can be mounted on a relocatable stable platform such as a ship or truck to facilitate magnetic surveying. In contrast to both ground-based and satellite-based measurements, the platform is not required to be magnetically clean or quiet.

The magneto-optical resonance manifests itself as a sharp increase in the returned fluorescence for the D2 line of sodium, or a decrease for the D1 line, as a function of the modulation frequency. The sodium fluorescence may be captured either by a single-channel photodetector or by an imaging array (e.g., a CCD camera); the latter allows additional background discrimination and the possibility of separately analyzing fluorescence signals from different altitudes if the imaging and laser-beam axes are not parallel.

### III. MEASUREMENT PARAMETERS

The magnetometric sensitivity of this technique is governed by the number of atoms involved in the measurement, the coherence time of the atomic spins, and the fraction of the total fluorescence intercepted by the detector, each of which we seek to maximize. A detailed discussion of mesospheric properties relevant to LGS has recently been given [8]. Briefly, the altitude of the sodium layer is  $\sim 90$  km, its thickness is  $\sim 10$  km, and sodium is present at a typical temperature of 180 K and a number density of around  $3 \times 10^9 \text{ m}^{-3}$ . This density is low by vapor-cell standards, but the interaction volume and hence the atom number can be quite large, limited chiefly by available laser power. The coherence time is limited primarily by collisions with other atmospheric molecules and secondarily by atom loss from the region being probed (e.g., due to diffusion or wind). A velocity-changing collision occurring after an atom is pumped typically removes the atom from the subset of velocity classes which are near-resonant with the laser light; as a consequence, these collisions result in an effective decay of spin polarization. Moreover, spin-exchange collisions of sodium atoms with unpolarized para-

magnetic species in the mesosphere, predominantly  $\text{O}_2$ , result in a randomization of the electron spin, and therefore also lead to decay of sodium polarization. To our knowledge, the spin-exchange cross-section of oxygen with sodium has not been measured, and in fact it is anticipated that measurement of mesospheric coherence times will more tightly constrain this important LGS parameter. However, its magnitude can be estimated from other known spin-exchange cross-sections, leading to an expected spin-damping time on the order of  $500 \mu\text{s}$ . The fraction of intercepted fluorescence is determined by the solid angle subtended by the detection telescope and the angular emission pattern of the fluorescing atoms; for a  $1\text{-m}^2$  telescope and isotropic emission, the fraction is approximately  $10^{-11}$  when the detector is directly below the fluorescing sample.

Sodium atoms in the mesosphere are distributed both in position and in velocity. They can be conceptually divided into velocity classes and spatial volumes, in each of which the collection of atoms functions approximately as an independent magnetometer. The width in velocity  $\Delta v$  of an individually addressable velocity class is set by the Doppler effect and the natural linewidth  $\gamma_0 \approx 2\pi \times 10 \text{ MHz}$  of the sodium transition. We can thus approximately calculate the sensitivity by calculating the evolution of a single sub-volume and velocity class; we then determine the total fluorescence by summing over sub-volumes and velocity classes. This approximate treatment is valid for length scales larger than the typical distance traveled by atoms in one coherence time, and for velocity classes that are approximately uncoupled. The latter condition requires that the laser intensity be low, so that radiation pressure is small, and that there be negligible probability of an atom begin transferred from one near-resonant velocity class to another by velocity-changing collisions.

The atom number can be maximized either by increasing the interaction volume or by including more velocity classes. Since the most probable atomic velocity component along the laser beam propagation direction is zero, broadening the laser spectrum to include velocity classes away from zero velocity will offer diminishing returns as spectral widths approaching the Doppler linewidth ( $\sim 1 \text{ GHz}$ ) are reached. By contrast, defocusing the laser beam to illuminate a larger region in space suffers no limitation other than the amount of laser power that can be supplied at a reasonable cost. For this reason, as well as for simplicity of implementation, defocusing the laser beam appears advantageous. If the observed relaxation due to velocity-changing collisions is significantly more rapid than that due to spin-exchange collisions, however, it may prove beneficial to broaden the laser spectrum to a width comparable to the Doppler linewidth, so that velocity-changing collisions will no longer cause loss of polarization but will merely cause atoms to be pumped and probed in different velocity classes.

### IV. RESULTS

One expects on intuitive grounds that the optimum laser intensity resonant with a single velocity class should be such that the characteristic rate of optical pumping  $\Gamma_p \equiv \gamma_0 I / 2I_{\text{sat}}$

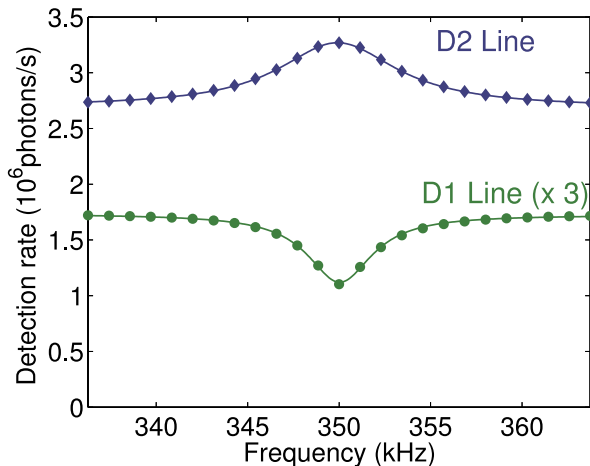


FIG. 2: Calculated magneto-optical resonance profiles for mesoscopic sodium. The resonances shown correspond to the D2  $F=2 \rightarrow F'=3$  (upper curve, blue diamonds) and D1  $F=2 \rightarrow F'=1$  (lower curve, green circles) sodium lines. The D1 curve has been multiplied by a factor of three to improve visibility. Symbols are the results of numerical calculations, and solid lines are Lorentzian fits to these results. Calculations are for an intensity  $I = 1 \text{ W/m}^2$  and a modulation duty cycle of 20% with a detector collection area of  $1 \text{ m}^2$ .

(where  $I$  is the laser intensity and  $I_{\text{sat}} \approx 60 \text{ W/m}^2$  is the saturation intensity of the sodium cycling transition) is on the same order as the decay rate of atomic polarization. For higher intensities, optical pumping will “reset” the precession before its coherence time has been fully exploited, while use of lower intensities sacrifices signal without improving the coherence time. We have performed a detailed ground-state density-matrix analysis of spin precession and optical pumping on the D1 and D2 transitions of sodium. In this analysis, we employ a circularly polarized pump laser beam oriented at right angles to a magnetic field of 0.5 G, with a spin-exchange collision time of  $500 \mu\text{s}$  and a velocity-changing collision time of  $200 \mu\text{s}$ . Since we employ optical intensities substantially lower than the saturation intensity, we expect the ground-state method to be accurate; we have also performed calculations of the resonance contrast for selected parameters using the full (ground and excited-state) optical Bloch equations. For a variety of settings of the pump light intensity and of the duty cycle (defined as the duration of a single pumping light pulse divided by the period of the modulation), we calculate resonance spectra as functions of the laser modulation frequency. Sample spectra for the laser tuned to the D1  $F = 2 \rightarrow F' = 1$  and the D2  $F = 2 \rightarrow F' = 3$  lines are shown in Fig. 2. From the width and peak height of these spectra, as well as the optical shot noise of the detected fluorescence, we calculate the magnetometric sensitivity. We assume that the noise is dominated by the fundamental shot noise and therefore neglect technical noise due to the photometric measurement. Contour plots of the sensitivity are shown as functions of the duty cycle and the laser intensity in Fig. 3 for the D1 and D2 lines.

In these calculations, a fixed number of velocity classes is considered (specifically fifteen, or five per excited-state hy-

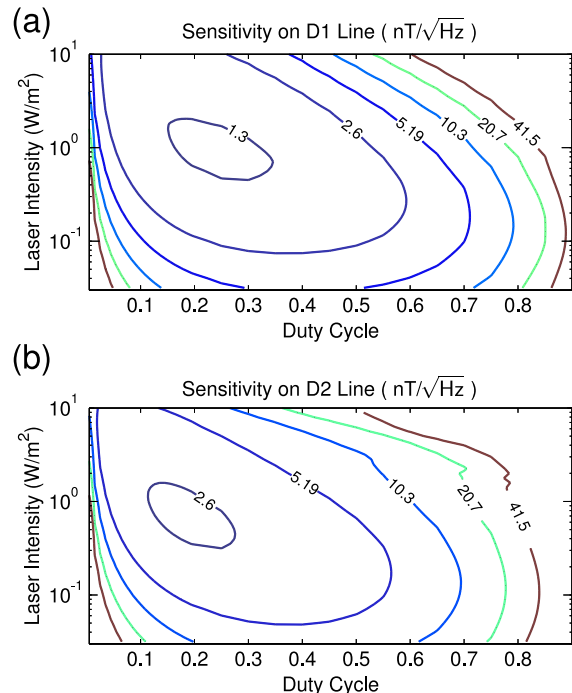


FIG. 3: Contour plot of calculated magnetometer sensitivity as a function of pumping duty cycle and intensity. Sensitivity is calculated including the hyperfine effect for the D2  $F=2 \rightarrow F'=3$  and D1  $F=2 \rightarrow F'=1$  lines, using a detector area of  $1 \text{ m}^2$ , a spin-exchange collision time of  $500 \mu\text{s}$ , and a velocity-changing collision time of  $200 \mu\text{s}$ . Contours are logarithmically spaced at intervals of one octave.

perfine component), and the effective laser beam size is adjusted to maintain a constant launched laser power of  $20 \text{ W}$  (typical of the latest generation of LGS lasers), which results in different numbers of participating atoms for different laser intensities. The optimum sensitivity of  $1.2 \text{ nT}/\sqrt{\text{Hz}}$  occurs on the D1 transition, at a duty cycle of 25% and pump intensity during each pulse of  $1.0 \text{ W/m}^2$ . The optimum intensity corresponds to an effective laser beam diameter in the mesosphere of around 5 m. This sensitivity is approximately one order of magnitude worse than the limit set by quantum spin-projection noise for the sodium atoms, presumably as a result of hyperfine structure and Doppler broadening. The optimum on the D1 line offers superior magnetometric sensitivity in part because the D1 resonances are dark, i.e., they result in a reduction of fluorescence, so that the photon shot noise is smaller and broadening of the resonance is reduced. If technical rather than fundamental noise sources dominate, then the D2 resonance may be preferable for its larger signal size.

We note also that the time scale of velocity-changing collisions is comparable to the relaxation time of the atomic spins, so that it is likely for a given atom to interact more than once with the laser light while remaining in a single velocity class. Thus the excited-state hyperfine structure is resolved throughout the pumping and probing process, and proximity

to a given ground-to-excited hyperfine transition can strongly influence the light-atom interaction[9]. For the same reason, magneto-optical resonances involving higher polarization multipoles such as alignment (which can be prepared by pumping with linearly polarized light) are expected to be observable in mesospheric sodium.

## V. ADDITIONAL EFFECTS

The magneto-optical resonance linewidth in mesospheric sodium is broader than in typical vapor-cell magnetometers; as a result, several effects important in vapor cells are less significant for mesospheric-sodium measurements. The quadratic Zeeman shift, for instance, leads to a splitting of the resonance into multiple resonances spaced by  $\sim 150$  Hz. However, since the width of the resonance at the optimum is around 5 kHz, this splitting will merely result in a small (and calculable) distortion of the lineshape. The natural inhomogeneity of the geomagnetic field will also affect the measurement, since the resonant frequency varies with altitude. Variation of the earth's field over the 10-km height of the sodium layer is on the order[10] of 100 nT, corresponding to about 700 Hz in Larmor frequency. Thus, although the modulation pumping laser cannot perfectly match the resonance frequency throughout the height of the mesosphere, this inhomogeneous broadening is again small compared to the width of the resonance at the sensitivity optimum. Consequently, we expect the effects of both the natural magnetic gradient and the quadratic Zeeman shift to be small. Temporal variations of the magnetic field in the mesosphere are, in principle, merely part of the signal being measured, and not an instrumental limitation. However, large enough fluctuations could make it difficult to track the resonance frequency. We take as a likely upper bound for the magnetic fluctuations on time-scales of 1 s to 100 s the typical observed value at the earth's surface under ordinary conditions of around 1 nT. As this is again substantially smaller than the resonance linewidth, we expect that except during magnetic storms, it should not be difficult to keep the laser modulation frequency on resonance. Variations of the height and density of the sodium layer itself are an additional practical concern. A realistic measurement will require reducing sensitivity to such variations through comparison of on-resonant and off-resonant signals, either by temporally dithering the modulation frequency or by employing spatially separated pump beams with different modulation frequencies.

A further deviation of the real experiment from the idealization embodied in the calculations comes from turbulence in the lower atmosphere, which causes random phase shifts

in distinct transverse patches of the laser beam. In the typical LGS application, the far-field diffraction (or speckle) pattern in the mesosphere from these low-altitude phase patches consists of elongated filaments whose individual lateral size is set by the numerical aperture of the laser launch telescope, but whose collective extent is governed by the size of the atmospheric patches[6]. Fluctuation of these filaments in time results in undesirable effects including random changes in pump-laser intensity in the mesosphere, motion of the illuminated column, and variation of the returned fluorescence. The relatively low intensity and large beam area indicated by our magnetometry calculations make such filamentation a lesser concern, however, since the beam diameter may be kept within the Fried length[11] of around 0.1 m in the most turbulent region of the lower atmosphere. Although lensing and beam-steering due to atmospheric variations will prevent precise fine-tuning of laser intensity, we do not anticipate that such variations will strongly affect the sensitivity obtainable with the proposed technique. We plan nevertheless to perform detailed modeling of atmospheric effects using physical optics, as has recently been done with reference to LGS [12].

## VI. CONCLUSIONS

In conclusion, we have presented a promising alternative to satellite missions for the measurement of geomagnetic fields. The proposed method requires only ground-based apparatus, and is consequently substantially less expensive per sensor than a satellite formation, while still achieving high magnetometric sensitivity. We anticipate that the low cost of deployment will make possible large-scale magnetic mapping and monitoring applications at the 100-km length scale, with temporal and spatial coverage that would be difficult to obtain by current techniques. Furthermore, as satellites cannot be operated as low as 100 km in altitude without excessive drag and heating, remotely-detected mesospheric magnetometry promises superior spatial resolution of terrestrial sources. In addition, the technique offers to supplement existing ground-based magnetic observatory data, allowing high-precision magnetic monitoring from a mobile platform without the requirement of a large-area, remote, and magnetically clean observation site on the earth's surface. We are currently constructing a 20-W-class laser projection system and working to implement this technique in proof-of-principle magnetic-field measurements.

The authors acknowledge stimulating discussions with Peter Milonni, William Happer, Michael Purucker, and Stuart Bale. This work is supported by the NGA NURI program.

---

[1] Campbell, W. H. An introduction to quiet daily geomagnetic fields. *Pure and Appl. Geophys.* **131**, 315–331 (1989).  
 [2] Tyler, R. H., Maus, S. & Luhr, H. Satellite Observations of Magnetic Fields Due to Ocean Tidal Flow. *Science* **299**, 239–241 (2003).

[3] Friis-Christensen, E., Lühr, H. & Hulot, G. Swarm: A constellation to study the Earth's magnetic field. *Earth, Planets, and Space* **58**, 351–358 (2006).  
 [4] Slavin, J. A. *et al.* Space Technology 5 multi-point measurements of near-Earth magnetic fields: Initial results. *Geophys.*

- Res. Lett.* **35**, 2107–+ (2008).
- [5] Purucker, M. *et al.* Magnetic field gradients from the ST-5 constellation: Improving magnetic and thermal models of the lithosphere. *Geophys. Res. Lett.* **34**, 24306–+ (2007).
- [6] Happer, W., MacDonald, G. J., Max, C. E. & Dyson, F. J. Atmospheric-turbulence compensation by resonant optical backscattering from the sodium layer in the upper atmosphere. *J. Opt. Soc. Am. A* **11**, 263–276 (1994).
- [7] Bell, W. E. & Bloom, A. L. Optically Driven Spin Precession. *Phys. Rev. Lett.* **6**, 280–281 (1961).
- [8] Holzlöhner, R. *et al.* Optimization of cw sodium laser guide star efficiency. *Astron. and Astrophys. preprint* (doi=<http://dx.doi.org/10.1051/0004-6361/200913108>).
- [9] Auzinsh, M., Budker, D. & Rochester, S. M. Light-induced polarization effects in atoms with partially resolved hyperfine structure and applications to absorption, fluorescence, and nonlinear magneto-optical rotation. *Phys. Rev. A* **80**, 053406 (2009).
- [10] National Geophysical Data Center. URL <http://www.ngdc.noaa.gov/geomagmodels/IGRFWMM.jsp>.
- [11] Fried, D. L. Optical resolution through a randomly inhomogeneous medium for very long and very short exposures. *J. Opt. Soc. Am.* **56**, 1372–1379 (1966).
- [12] Holzlöhner, R., Calia, D. B. & Hackenberg, W. Physical optics modeling and optimization of laser guide star propagation. vol. 7015, 701521 (SPIE, 2008).